ACS OMEGA

http://pubs.acs.org/journal/acsodf

Article

Ketoconazole-Loaded Cationic Nanoemulsion: *In Vitro*–*Ex Vivo*–*In Vivo* Evaluations to Control Cutaneous Fungal Infections

Mudassar Shahid, Afzal Hussain, Azmat Ali Khan, Mohhammad Ramzan,* Ahmed L. Alaofi, Amer M. Alanazi, Mohammad M. Alanazi, and Mohd Ahmar Rauf

Cite This: *ACS Omega* 2022, 7, 20267–20279

Read Online

ACCESS | Metrics & More | Article Recommendations

ABSTRACT: An attempt has been made to optimize ketoconazole (KTZ)-loaded cationic nanoemulsion for topical delivery followed by *in vitro*, *ex vivo*, and *in vivo* evaluations. Central composite design suggested a total of 13 outcomes at 3 factors and 2 levels against 6 responses. Formulations were characterized for globular size, polydispersity index, pH, ζ potential, % entrapment efficiency (% EE), and drug content. Moreover, the optimized KTZ-CNM13 was compared against drug suspension (KTZ-SUS), commercial cream, and anionic nanoemulsion for *in vitro* drug release, *ex vivo* permeation, *in vitro* hemolysis, antifungal assay, *in vivo* dermal irritancy, and long-term stability. KTZ-CNM13 was found to have a low size (239 nm), an optimal ζ potential (+22.7 mV), a high % EE (89.1%), a spherical shape, a high drug content (98.9%), and a high numerical desirability value (1.0). *In vitro* drug release behavior of KTZ from KTZ-CNM13 was 7.54- and 1.71-folds higher than those of KTZ-ANM13 and KTZ-SUS, respectively, at 24 h. The permeation rate values were ordered as KTZ-CNM13 > KTZ-ANM13 > KTZ-MKT > KTZ-SUP due to various studied factors. High values of zone of inhibition for KTZ-CNM13 were observed against *Candida albicans*, *Candida glabrata*, *Candida tropicalis*, and *Candida krusei* as compared to KTZ-SUS. *In vitro* hemolysis and *in vivo* irritation studied confirmed the safety concern of the nanoemulsion at the explored composition. Long-term stability result revealed a stable product at the explored temperature for a year. Conclusively, cationic nanoemulsion is a promising approach to deliver KTZ for high permeation and therapeutic efficacy.

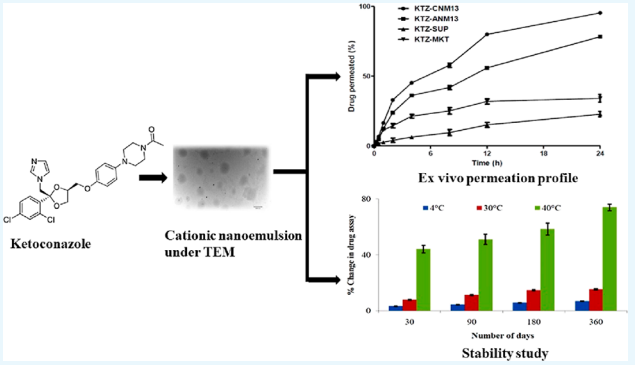

INTRODUCTION

Developing and under-developed countries are more prone to fungal (*candida* and *aspergillus* species) infections (40 million) annually, and these are identified as progressive coinfection with the virus in France (20%), Germany (26.3%), the Netherlands (19.4%), and China (5–15%).[1,2] Ketoconazole (KTZ) is a broad spectrum antifungal azole with limited aqueous solubility (0.3 mg/mL), high plasma protein binding capacity (84%), and limited oral delivery (common to control onychomycosis infection as 14% of the population) to control local and systemic fungal infections.[3−5] Topical therapy is still a mainstay to treat fungal infections of the deep-seated pathogen and persistent nature of the infection with minimum side effects (reactions associated with oral delivery) and high patient compliance by localized drug access. Moreover, topical delivery results in direct, localized delivery of KTZ to the infected site at a low cost burden.[5] Several antifungal drugs have been explored for improved topical delivery using nanotechnology-based novel carrier in the literature. Similarly, KTZ has been investigated for improved topical delivery using various strategies, and these are novel lacquer formulation (transungual delivery), herbal liposomes, niosomal gel, solid lipid nanoparticle-based hydrogel, and liposomes.[6−10] Conventional dosage forms intended for topical application are challenged with inefficient delivery, insufficient permeation across skin, and poor efficacy due to subtherapeutic level achieved in the deeper layer of the skin. Considering our recent published findings, *in vivo* dermacokinetics parameters of the optimized solid lipid nanoparticles (KTZ-SLN4) were improved by 410−900% as compared to commercial Nizral (2%) using solid lipid nanoparticles of 291 nm and % entrapment efficiency (% EE) of 85%.[10] Furthermore, mechanistic evaluations of KTZ-SLN4 were explored for improved efficacy, enhanced topical penetration, cellular uptake (L929 and J774A.1), and safety assessment in *in vitro*

Received: April 9, 2022
Accepted: May 20, 2022
Published: May 30, 2022

Table 1. Composition and Optimization of Various Selected Material Attributes and Corresponding Responses of Ketoconazole-Loaded Cationic Nanoemulsion Formulation Containing a Fixed Amount of OLA (0.02% w/v) as a Cationic Charge Inducer[a]

formulation	CAP (%w/w)	S_{mix} ratio (LAB/PG)	water content (% w/w)	particle size (nm)	PDI	pH	ZP (mV)	EE (%)	drug assay (%)
	independent variables			dependent variables					
runs	X_1	X_2	X_3	Y_1	Y_2	Y_3	Y_4	Y_5	Y_6
KTZ-CNM1	15.5	2:1	53	275 ± 3.8	0.35	7.6	+16.2	81.2 ± 0.3	94.5 ± 0.7
KTZ-CNM2	10.5	2:1	42	295 ± 4.7	0.41	7.3	+11.3	78.9 ± 0.4	93.2 ± 0.2
KTZ-CNM3	12.5	2:1	47	286 ± 8.4	0.31	7.5	+19.6	76.5 ± 0.7	91.8 ± 0.3
KTZ-CNM4	12.5	1:1	42	288 ± 5.5	0.33	7.2	+21.9	83.6 ± 1.1	94.5 ± 0.3
KTZ-CNM5	12.5	3:1	42	269 ± 5.2	0.32	7.3	+17.9	80.9 ± 0.8	90.2 ± 0.6
KTZ-CNM6	12.5	1:1	53	299 ± 1.9	0.36	7.8	+18.4	83.1 ± 0.2	90.4 ± 0.8
KTZ-CNM7	15.5	2:1	53	310 ± 7.5	0.38	7.7	+15.6	81.2 ± 0.3	92.5 ± 0.7
KTZ-CNM8	10.5	1:1	47	276 ± 5.3	0.41	7.9	+17.8	80.3 ± 0.7	96.3 ± 0.5
KTZ-CNM9	15.5	1:1	47	397 ± 6.2	0.44	7.6	+14.9	82.5 ± 0.9	91.9 ± 0.9
KTZ-CNM10	10.5	2:1	47	402 ± 8.9	0.39	7.5	+20.6	82.7 ± 0.6	92.3 ± 1.2
KTZ-CNM11	12.5	2:1	47	289 ± 2.4	0.32	7.7	+21.3	82.9 ± 1.3	90.7 ± 1.5
KTZ-CNM12	12.5	3:1	47	293 ± 1.4	0.28	7.2	+23.5	82.0 ± 0.5	94.3 ± 0.7
KTZ-CNM13#	12.5	2:1	53	239 ± 5.2	0.24	7.4	+22.7	89.1 ± 1.4	98.9 ± 0.9
KTZ-ANM13#	12.5	2:1	53	245 ± 3.3	0.26	7.3	−26.6	84.7 ± 0.2	95.4 ± 0.7

[a]KTZ = ketoconazole, CAP = Capmul PG8, PDI = polydispersity index, ZP = ζ potential, EE = entrapment efficiency, PG = propylene glycol, and LAB = labrasol.

and *in vivo* investigations. Results showed improved antifungal efficacy (70−95%) by reducing the minimum inhibitory concentration (MIC, 50−75% reduction) than the suspension. Notably, cellular uptake was augmented 12.6-fold higher than the suspension which may be correlated with lipid−lipid internalization between the fungal cell membrane/dermal cell lines and the SLN4 nanocarrier.[11] Cationic charge inducer can be used to impart electrostatic interaction between the negatively charged cell membrane (human, fungal, and bacteria) and the nanocarrier during absorption and exposure with fungal cells.[12] Oleylamine (OLA) is a cation charge inducer, remains fully ionized at pH 5−6 at the interface (nanoemulsion globules), and produces homogeneous size distribution at a low concentration (0.05%).[13] OLA is a hydrophobic lipid (log p = 7.6) with a low molecular weight (267.5 g/mole) to impart cationic charge for ophthalmic drug delivery (emulsion) at the tolerance dose of 1 mg/mL in a rabbit for 28 days.[14]

Our ongoing research was further extended for exploitation of cationic nanoemulsion-based KTZ delivery to control local, onychomycosis, and deep sited (dermal site) fungal strains. The design was hypothesized based on the remarkable findings reported before and the theoretical concept. In order to facilitate enhanced topical permeation of KTZ, it was mandatory to consider several aspects in the formulation design, and these are optimized size, drug solubilization in the nanocarrier system, added electrostatic interaction between cells and nanocarriers, induced reversible structural changes in the skin barrier, and physicochemical stability for the shelf-life period. Several reports (transdermal and ophthalmic) claimed successful delivery of lipophilic drugs using cationic nanoemulsion to achieve expected outcomes such as high drug EE, enhanced permeation profiles, increased therapeutic efficacy, high patient compliance, low cost burden, and ease in scale up for large-scale production.[15−17]

MATERIALS AND METHODS

Materials. KTZ (>95% pure) was kindly gifted by Hitech Formulations Pvt. Ld. Chandigarh (India). Capmul PG 8 (CAP) was obtained from Abitec Corporation (Janesville, Germany). Propylene glycol (PG), tween 80, and polyethylene glycol 400 (PEG400) were procured from Avarice Laboratories, Ghaziabad (India). Solvents such as dimethyl sulfoxide (DMSO) and methanol (analysis grade) were purchased from SD Fine, Mumbai, India. Labrasol is a chemically combined content of caric and caprylic acid (LAB) (Gattefosse, Saint Priest Cedex, France). OLA as a positive charge inducer was purchased from Sigma-Aldrich, India. Cultures were obtained from the Indian Institute of Microbial Technology, Chandigarh, Punjab, India. Materials used in the experiments were of analytical grade and used as such.

Methods. *Solubility Studies.* KTZ is poorly soluble in aqueous or neat water solution. However, the solubility study was conducted in various excipients.[18] KTZ belongs to a biopharmaceutics classification system class II with very slight solubility in acetate buffer (0.3 mg/mL). Therefore, it was required to analyze the solubility of KTZ in various excipients, viz., oil, surfactant, and cosurfactant, to identify the best excipients for formulating the cationic nanoemulsion. Briefly, KTZ was solubilized in each component (5 mL) in a stopper glass vial (10 mL) and stirred (10.0 min) at room temperature (28 ± 1 °C). Each sample was kept in a shaking water bath at a constant temperature (28 ± 1 °C) and shook for 72 h. After a predetermined time, each centrifuged and filtered sample was chemically analyzed using a UV−vis spectrophotometer (UV-1280, Shimadzu Corporation, Japan) at 242 nm (n = 3) after dilution (methanol).

Optimization Process and Desirability Function. In this study, the experimental design tool was used to identify the critical factors (X_1−X_3) and their significant levels to optimize the desired content of oil (CAP as X_1), S_{mix} ratio (LAB/PG as X_2), and aqueous content (water as X_3). A central composite design (CCD) was run in the Design Expert (version 8.0.1

https://doi.org/10.1021/acsomega.2c02219
ACS Omega 2022, 7, 20267−20279

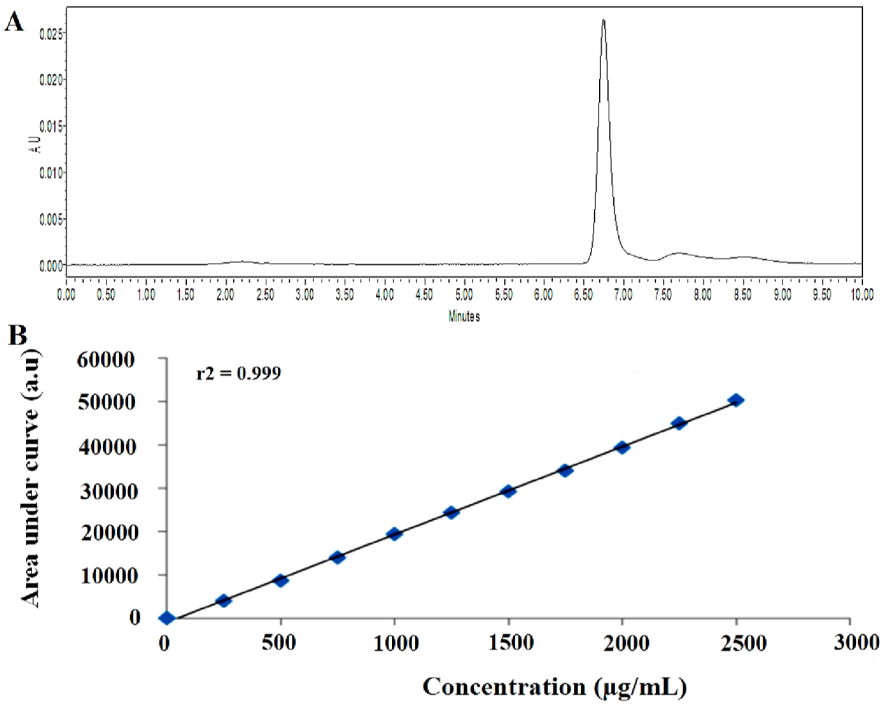

Figure 1. HPLC chromatogram of KTZ shows the retention peak time at 6.67 min (A) and the calibration curve of KTZ at a concentration range of 0.25−25 μg/mL (B).

Stat-Ease Inc. United States of America) by adopting X_2 and X_3 as independent factors against six dependent variables (response variables, Y_1−Y_6). A similar design was conducted and reported by us before.[10] Similarly, the mean particle diameter (Y_1), polydispersity index (PDI) (Y_2), pH (Y_3), ζ potential (ZP) (Y_4), % EE (Y_5), and drug assay (Y_6) were set responses (dependent variables) under provided constraints (targeted, minimum, maximum, and in range). Constraints were set as per optimization process to get maximum desirability (numerical functional validation parameter). A total of 13 runs gave various combinations of X_1, X_2, and X_3 during the optimization process. A combination revealing maximum desirability was reformulated and characterized for the set responses. Table 1 shows various combinations of factors against the studied responses. Functional desirability value may range from zero to unity. Zero indicates the failure of optimization under set conditions or out of design/model for a study.[11]

Preparation of KTZ-Loaded Cationic Nanoemulsion (KTZ-CNM). Initial screening of developed formulation was based on the benchtop stability (overnight) in order to select suitable excipient and respective levels (low and high) of each factor. Based on the benchtop stability product, levels were fixed (high or low) to use as an input parameter in the experimental design software. Formulations were prepared by dissolving KTZ in CAP containing OLA (positive charge inducer) due to the highest solubility which served as an organic phase. The clear organic phase was slowly titrated with the aqueous phase containing S_{mix} ratio (LAB/PG). Thus, various formulations were prepared as suggested in the experimental design (CCD). Then, oil in water (o/w) nanoemulsion was obtained by selecting the optimized concentrations of surfactant and cosurfactant in pseudo-ternary phase diagrams (not shown here). Briefly, the developed formulations were kept at 25 ± 2 °C for 24 h under constant physical observation. A formulation was dropped from further investigation if any signs of instability (color, phase separation, creaming or precipitation) were observed. Several formulations (KTZ-CNM1 to KTZ-CNM13) were optimized for selecting a suitable ratio of surfactant to cosurfactant concentration based on physical observation by subjecting to benchtop stability. Thus, the most suitable ratio of S_{mix} was optimized as 2:1 due to the maximum delineated area in the phase diagrams. Finally, these cationic nanoemulsions were further characterized for globular size, PDI, and ZP before final selection of the most optimized cationic nanoemulsion. Each formulation contained 20 mg per mL of KTZ (2%). In the case of KTZ suspension (KTZ-SP), it was prepared in carboxymethyl cellulose (1% w/v) by stirring for 1 h to use as control.

Globular Size, PDI, ZP, and pH Measurement. Physical characteristics of each formulation were expressed in terms of size, ZP value, and PDI values. Globular size, size distribution in terms of intensity (PDI), and surface charge density (ZP) were estimated after loading the drug. Each sample was diluted before globular and PDI analyses to avoid size analysis error. However, ZP values were determined without dilution to find real-time estimation of ZP of formulations. Thus, the globular size and PDI values were estimated using the diluted (Milli-Q water about 50 times) sample and analyzed by an analyzer (Beckman Coulter, Delsa Nano C, United States of America). In this study, OLA was anticipated to be adhered as a surface charge inducer which subsequently may result in a positive charge (ZP) for electrostatic repulsion amid nanoglobules of bulk formulation.[18] On the other hand, the undiluted samples were used to measure real-time ZP values at room temperature (Zetasizer Delsa Nano C, United States of America). The study was replicated for mean and standard values (n = 3). Furthermore, pH was measured using a digital pH meter (PICO pH meter, Lab, India Analytical, India). Few supportive evaluation parameters were estimated for the optimized

https://doi.org/10.1021/acsomega.2c02219
ACS Omega 2022, 7, 20267−20279

formulation, and these were (a) pH (calibrated digital pH meter), (b) refractive index (using a Fisherbrand refractometer, Fisher Scientific, USA), and (c) % transmittance (using a spectrophotometer).

Quantification of KTZ Using HPLC Method. The drug content was estimated using validated high-performance liquid chromatography (HPLC) technique (Waters, empower 2.0, USA) as reported before by us.[10] A standard plot was prepared, and the quantity of the drug was analyzed using a reverse phase column "C_{18}" (150 mm × 46 mm, 5 μ particle size) at an operating column temperature of 30 ± 1 °C. The used mobile phase was set for complete resolution and the desired retention time [acetonitrile and phosphate buffer (pH 4.4) in the ratio of 1:1]. An optimized volume of the sample was injected (20 μL) at a flow rate of 1 mL/min, a run time of 10 min, and a peak retention time at 6.76 min. KTZ was quantified at 230 nm using a photodiode array (PDA) detector, and the column temperature was maintained at 45.3 °C throughout the analysis. For the calibration curve, dilutions were prepared in methanol in the concentration range of 0.5−25 μg/mL, and a graph was plotted between concentration versus AUC (area under curve) at a regression coefficient (r^2) of 0.999 (Figure 1A,B). The analysis was replicated to get mean and standard deviation (n = 3).

% EE. The values of % EE were estimated for the optimized nanoformulations (KTZ-CNM1- KTZ-CNM13). Briefly, the sample (0.1 mL) in the dialysis membrane was initially stirred for 30 min using methanol (50%) as a dialysis solvent. The free drug was released into the dialysis solvent medium, and the remaining content was completely dissolved in a mixture of chloroform and methanol (2:1). Both of them were analyzed for the drug content using the validated HPLC method and a PDA detector. The values of % EE were estimated using the following mathematical equation

$$\% \text{ EE} = (C_i - C_f) / C_i \quad (1)$$

wherein C_i and C_f are the initial concentrations of the drug and the final drug content estimated, respectively.

Drug Assay/Total Drug Content. In order to estimate the total drug content (TDC), each formulation was separately studied (KTZ-CNM1 to KTZ-CNM13). In brief, the formulation to be tested was first solubilized in a mixture of methanol/chloroform (1:2) for 60 min under constant magnetic stirring. Then, the mixture was rigorously vortexed for 5 min at 25 °C to ensure complete mixing of the dissolved amount of the drug. Finally, the mixture was centrifuged, and the filtrate was used to analyze the drug content using the previously developed HPLC method.[10] Each sample was replicated.

Globular Morphology (Microscopic Analysis). The morphology (size and shape) of the optimized KTZ-CNM13 was scanned by an advanced and sophisticated transmission electron microscopy (TEM) technique. The technique is more reliable and well established to view the nanocarrier under high resolution. In brief, a drop of nanoemulsion formulation was placed on a grid followed by drying and negative staining. In general, the wet sample is not well scanned and causes deviation of the electron beam while processing. Therefore, we completely dried the sample before analysis. KTZ-CNM13 was first diluted using distilled water (50X) and then scanned using high-resolution TEM (HR-TEM) for well-resolved images. Notably, the sample needs to be stained using a negative staining agent (phosphotungstic acid, 0.2%) and left for drying (overnight). The completely dried sample was easily scanned without any interference with the electronic beam (used as a source of light). The sample was finally spread on the copper grid and coated with carbon to make it conductive under an electron beam of HR-TEM (H-7500, Hitachi, Japan) at a voltage of 200 kV.[19]

In Vitro Drug Release Study. *In vitro* release behavior of KTZ-CNM13, KTZ-ANM13, and KTZ-SUP was studied using a dialysis membrane (12 kDa molecular weight cutoffs, HiMedia, Laboratories, Pvt., Mumbai, India) as per the reported method.[10,20] The dialysis membrane was first soaked in PBS (phosphate-buffered solution) solution to activate the membrane at room temperature for 24 h. Each formulation (containing 20 mg of KTZ) was packed in a dialysis bag and tightly closed from both sides. The sample loaded dialysis bag was submerged in a beaker containing PBS 7.4 and DMSO (0.5%) (maintained sink condition). Sampling was performed at varied time points, and an equal volume of the sample was replaced with fresh release media (0.5, 1, 2, 4, 8, 12, and 24 h) to maintain the volume of the receiving beaker. The withdrawn sample was filtered using a membrane filter and assayed using HPLC with a PDA detector after suitable dilution.[10] The release mechanism was evaluated by applying different mathematical models (zero order, first order, Higuchi and Korsemeyer-Peppa's model).

Ex Vivo Release Study Across Rat Skin. Skin permeation potential was determined using the earlier reported method from rat skin, and the abdominal male rat skin was employed (albino) (230−260 g; 12−14 weeks) after ethical sacrifice of animals (cervical dislocation).[21] All of the animals were received from the department and approved from the institute (PU/45/99/CPCSEA/IAEC/2018/150) committee of Panjab University, Chandigarh, India. The approved procedure, protocol, and method complied with the ARRIVE guidelines and the EU Directive 2010/63/EU. The skin was made free from hairs by shaving. The skin was processed to make free of fatty debris and fats using a surgical tool. To avoid any chemical mediated changes, no chemical remover was used. The cleaned skin was properly installed between the donor and acceptor chambers of the Franz diffusion cell. The epidermis faced the loaded sample, whereas the dermal side of the skin was facing the acceptor medium (PBS, pH 7.4). The receptor chamber was kept under regular stirring using an inert rice bead. KTZ-CNM13, KTZ-ANM13, KTZ-SUS, and KTZ-MKT (Nizoral; Janssen Pharmaceuticals) were investigated under the same experimental conditions for 24 h at 37 °C. The sample was collected using an injection syringe at each time point (0.5, 1, 2, 4, 8, 12, and 24 h), and an equal volume was used to replace the withdrawn sample. The permeated amount of the drug was estimated using the HPLC method and compared with the drug suspension.[10,11] The experiment was repeated to get mean and deviation (n = 3).

Drug Deposition Study. This study was based on the *ex vivo* permeation experiment. After the completion of *ex vivo* permeation study, the treated skin was carefully removed from the diffusion cells, and then the adhered sample was removed from the surface using running water. Each treated skin was excised from the loaded skin in such a way that only the exposed and passively operating surface (exposed circular area) was removed using a surgical scissor. The active surface area was cut into small pieces and placed in a solution of methanol/chloroform (1:2). The deposited drug was extracted by exposing the sliced skin in the same solution for 12 h under

https://doi.org/10.1021/acsomega.2c02219
ACS Omega 2022, 7, 20267−20279

constant magnetic stirring. After 12 h, the sample was homogenized and centrifuged to remove tissue debris. The supernatant was used for drug content estimation using the HPLC method.[10]

Antifungal Activity of the Optimized Formulations. *In vitro* antifungal assay of different formulations (KTZ-CNM13 and KTZ-ANM13) was performed against *Candida albicans* (*C. albicans*) and their clinical resistant strains [*Candida glabrata* (*C. glabrata*), *Candida tropicalis* (*C. tropicalis*), and *Candida krusei* (*C. krusei*)] at the reported MIC values. The experimental protocol was duly approved from Institutional Biosafety Committee of Panjab University, Chandigarh, India. Briefly, the nutrient agar media was prepared, and fungal organisms were inoculated. After solidifying the growth media, wells were prepared by a sterilized steel borer. KTZ-CNM13 and KTZ-ANM13 were serially diluted using sterilized water for injection, and the desired set concentration was transferred to the respective labelled well. Placebo KTZ-CNM13 and KTZ-ANM13 were also taken as the test samples. Finally, each Petri dish was properly labelled and sealed using the paraffin film to avoid cross-contamination and from drying during incubation at 37 °C for 48 h. After completion of 48 h, the zone of inhibition (ZOI) was measured using a scale, and the mean value was reported.[22] Any cross-contaminated Petri dish was not considered in the study.

Hemolytic Toxicity. Red blood cellular toxicity of the developed formulations (KTZ-CNM13 and KTZ-ACM13), blank KTZ-CNM13, blank KTZ-ACM13, KTZ-SUP, positive control (triton-X-100), and negative control (PBS) was investigated after exposing of red blood cells (RBCs) with each individual formulation. Briefly, each sample was properly diluted to a concentration of 1.25 and 2.5 μg/mL and exposed to interact with 4% RBC suspension. Each mL of the sample and RBC suspension was transferred to a previously sterilized tube containing the anticoagulant. The final volume was made up to 4 mL using PBS solution. This was a preliminary toxicity assessment at this stage due to the sensitivity of RBCs circulating in the blood. A similar procedure was adopted for the control groups. Positive control was anticipated to cause hemolysis due to extraction of RBC membrane protein and lipid. Negative control was used for comparison and expected to cause serious RBC damage or hemolysis due to optimal osmolarity and physiological pH. The tube was tightly closed and gently shaken to mix RBC cells for interaction. Each was placed in the incubation chamber for 2 h at 37 ± 1 °C. Then, each tube was carefully withdrawn and centrifuged (8000 rpm) to separate the debris, and the supernatant was used to estimate the released hemoglobin. The absorbance was taken using a UV−vis spectrophotometer (UV-1601, Shimadzu) at 540 nm (λ_{max}).[23]

In Vivo Acute Dermal Toxicity Study. The developed formulation was intended for topical application to control superficial and deeply residing fungal cells. The excipients were biocompatible at the explored concentration and were nonsensitive to the skin. However, it was mandatory to ensure that they are compatible and are free from any sensitivity reactions (irritation, edema, and inflammatory reaction) after topical application. Draize test is recommended to negate irritation behavior of any formulation using the rabbit or rat model. Rabbits were caged as per the standard laboratory conditions [20−25 °C and 55−65% relative humidity (RH)] to acclimatize in the condition prior to initiating the experiment. In this study, a white albino rabbit weighing approximately 1.5−2.0 kg (either sex) was selected and inspected for any dermal abnormality. On the back side of each rabbit, three circles (1.5 cm^2 each) were prepared by removing the hairs and marked using a marker. Groups and doses of various formulations were as follows: negative control group (0.3 mL of phosphate buffer at pH = 7.4), positive control group [0.3 mL of sodium dodecyl sulfate (SDS) 1% w/v], placebo (blank KTZ-CNM13) test group, and 0.3 mL of nanoemulsions KTZ-CNM13 and KTZ-ANM13 with the drug. The applied site was saved (covering with net) from the reach of rabbit legs or licking tongue after slight irritation or discomfort feeling. The treatment site was physically inspected for any sign of edema, toxicity, inflammation, and swelling till 24 h.[24] Results were presented as score.[25] Responses were defined in terms of average score as per the reported method.[25]

Long-Term Stability. Based on *in vitro* and *ex vivo* findings, the optimized cationic nanoemulsion (KTZ-CNM13) was finally opted as the most optimized formulation. The same was subjected for long-term stability as per ICH guidelines (Q1A). Generally, the nanoemulsion is prone to physical instability on long-term storage due to Ostwald ripening.[26] The imposed cationic nanoemulsion and substantial surfactant rendered more stability due to electrostatic repulsion existing among nanoglobules and the stern surfactant-based layer coated over globules. Properly packed and labelled formulation KTZ-CNM13 was placed in a stability chamber at a refrigerator temperature (2−8 °C) and 30 ± 2 °C/65 ± 5% RH for a year. KTZ-CNM13 was assessed for size, PDI, and % EE after 90, 180, and 360 days.[27]

Statistical Analysis. Collected data from experimental studies were calculated, analyzed, and interpreted using suitable mathematical models and statistical parameters. A significant variation was considered at $p < 0.05$ and $p < 0.001$ as described in the text body. The generated raw data were processed using software, and graphical presentation was illustrated in the figure using GraphPad prism (version 5.01, GrapPad software, Inc., La Jolla, CA). Experimental design (Design Expert) tool was used to optimize the factor and level for the desired outcome based on the desirability numerical functional statistical value and statistical model such as one-way ANOVA (analysis of variance) followed by Tukey (Sigma Stat Software, 2.03).

RESULTS AND DISCUSSION

Solubility Analysis and Optimization Process. The selection of various excipients was based upon the maximum solubility of KTZ. It was reported that KTZ is a lipophilic drug (log P = 4.35) with low aqueous solubility (13 μg/mL at 25 °C). Being poorly aqueous soluble, the study was rationalized to select suitable excipients (oils, surfactant, and cosurfactant) for stabilized nanoemulsion formulation. The solubility values obtained in the explored excipients (oils, surfactants, and cosurfactants) are depicted in Figure 2A along with its molecular structure "(1-[4-[4-[[2-(2,4-dichlorophenyl)-2-(imidazole-1-ylmethyl)-1,3-dioxolan-4-yl]methoxy]phenyl]-piperazin-1-yl]ethanone)" (Figure 2B). Maximum solubility was obtained in Capmul PG8 (74.32 ± 1.3 mg/mL) followed by labrasol (54.53 ± 1.36 mg/mL) and PG (29.28 ± 1.45 mg/mL). Lower values of KTZ solubility were observed in water (0.75 mg/mL ± 0.2), Transcutol (1.37 ± 0.4 mg/mL), and ethyl acetate (2.21 ± 0.98 mg/mL).

However, Capmul PG8, Lab, and PG were selected for further optimization process. OLA was used to impose positive

https://doi.org/10.1021/acsomega.2c02219
ACS Omega 2022, 7, 20267−20279

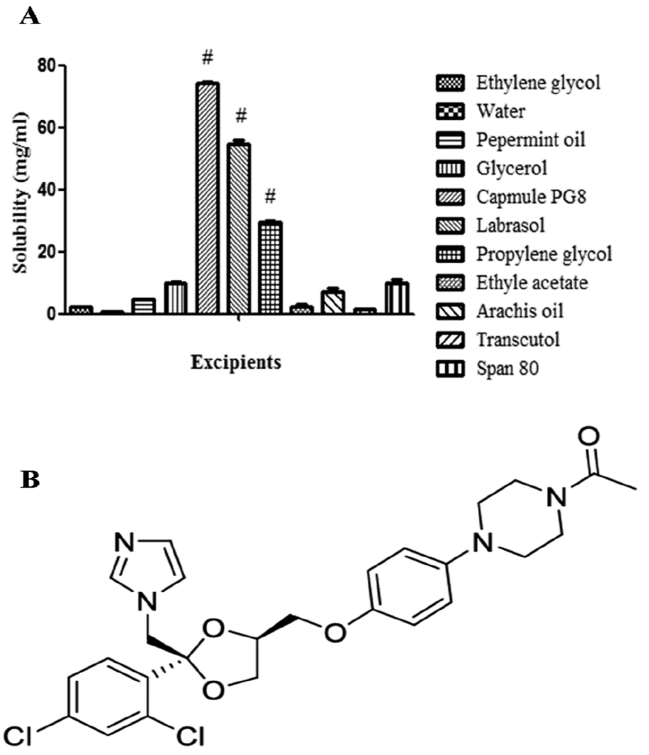

Figure 2. Solubility of KTZ in various oils, surfactants, and cosurfactants (A) and chemical structure of KTZ (B).

(cationic) charge on the nanoformulation which increases the electrostatic interaction between the nanoformulation carrier and the cell wall of fungal hyphae (negative charge). Several batches of KTZ-loaded nanoemulsion formulations were prepared by varying the amount of Capmul PG8, Lab, PG, and water (Table 1) using CCD, and 13 compositions were predicted under set constraints and goal (Table 1). KTZ-CNM13 exhibited the lowest globular size (292 nm), optimum charge on surface (ZP ~ +22.7 mV), highest % EE (89.1 ± 1.4), and highest % drug assay/TDC (98.9 ± 0.9). Figure 3 depicts that the overall desirability for applied design is maximum (desirability: 1.0).

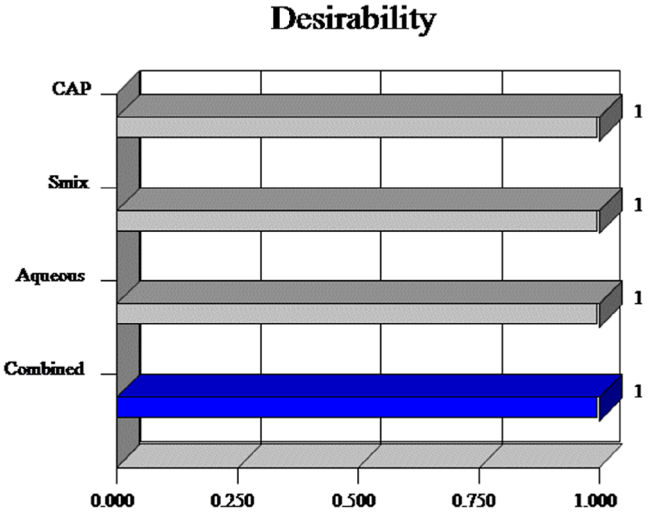

Figure 3. Desirability profile of KTZ-CNM using CCD design.

Characterization of Optimized KTZ-Loaded Nanoemulsion. *Microscopic Analysis.* It is a well-known fact that the globular size, PDI, and shape play an important role for drug absorption, permeation, and detrimental effect against pathogenic strains. The spherical shape of the globular/particle is considered as the most ideal morphology for maximum absorption. Therefore, TEM result confirmed the spherical nature of the optimized formulation and well dispersed in the bulk. This may be prudent to correlate with the imposed cationic charge for positive ZP keeping globules well dispersed without any agglomerates or Oswald ripening. Microscopic image of KTZ-CNM13 is depicted in Figure 4A wherein the HR-TEM result shows the spherical nature of optimized KTZ-CNM13 free from any aggregation, well-dispersed globules, and homogeneous nature of size distribution (Figure 4B) within the scanned region. Nonaggregation of the globules indicated an optimized concentration of the surfactant and cosurfactant which suitably prevented their coalescence on contact.[25] Electron microscopic study clearly confirmed the spherical nature of the lowest globular size of KTZ-CNM13, suggesting maximized adherence to the fungal cell wall for augmented internalization and subsequent detrimental consequences in fungal cells. Furthermore, the particle size and spherical behavior of nanoglobules facilitate antifungal efficacy of the drug due to the increased surface area and ease of cellular internalization with the nanocarrier to treat infections and recurrence cases.[28]

% EE, Drug Assay, % Transmittance, and Reflectance. % EE of optimized formulation showed high value (89.9% ± 1.4) of entrapped drug as compared to other formulations. Furthermore, the drug assay/TDC was also the highest (98.9 ± 0.9%) in optimized nanoemulsion (KTZ-CNM13). Results of % transmittance (% T) and total reflectance obtained from various formulations are shown in Figure 5. There was no significant ($p < 0.05$) difference in % T in all formulations (KTZ-CNM1-KTZ-CNM13), and values are from 91.3−94.7. No significance ($p < 0.05$) change was observed in total reflectance values (1.3−2.7). These values suggested stable, transparent, and kinetically stable cationic nanoemulsion at the explored temperature, viscosity, and composition. However, these parameters may vary on standing for a prolonged time and storage conditions. Therefore, these evaluations would be considered for long-term stability at varied temperature and RH for successful commercialization.

***In Vitro* Release Profile.** Physical nature of KTZ is highly crystalline, and it is poorly soluble in aqueous media (0.04 mg/mL). *In vitro* release behavior of KTZ-CNM13, KTZ-ANM13, and drug suspension (KTZ-SUP) was determined, and the results are depicted in Figure 6. The release of the drug from KTZ-CNM13 was significantly at a controlled rate (95% release at 24 h) in PBS (pH 7.4) containing 5% (v/v) methanol in comparison to KTZ-SUP (12.6 ± 0.8% release at 24 h). However, the anionic formulation (KTZ-ANM13) exhibited slow release (55.6 ± 0.69% release at 24 h) which may be due to the absence of free amino groups present on the nanoglobular surface as observed in the cationic nanoemulsion. OLA is reported to interfere with oily droplets by changing the orientation of the surfactant and cosurfactant in the bulk and coated barriers among globules for improved drug solubilization and stability in cationic nanoemulsion by interacting in many ways (dipole−dipole, hydrogen bonding, and van der Waals interaction).[29,30] In the cationic nanoemulsion, the role of OLA and other surfactant is to form a basic requirement for

https://doi.org/10.1021/acsomega.2c02219
ACS Omega 2022, 7, 20267−20279

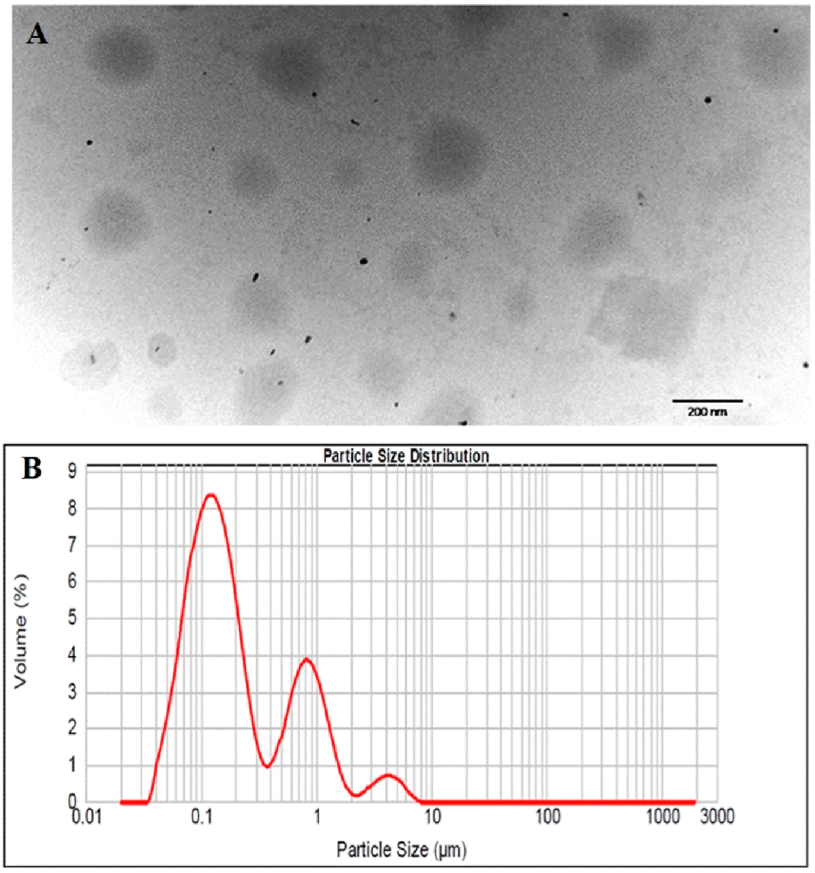

Figure 4. (A) Morphological assessment using TEM and (B) particle size distribution of optimized formulation.

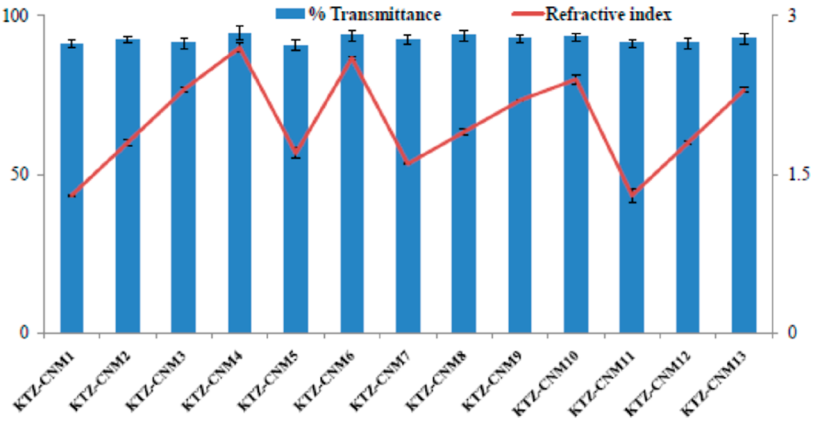

Figure 5. % T in various formulations and total reflectance of various formulations (KTZ-CNM1-KTZ-CNM13).

globular stabilization with reduced energy and stable orientation. OLA also served as the surfactant at a low concentration by binding with the lipid surface through the amino head group forming a stable outer layer on the surface.[30] KTZ-CNM13 and KTZ-ANM13 demonstrated 620 and 490% maximum KTZ release than KTZ-SUP. This may be due to poor solubility of KTZ in the water-based suspension. Figure 6 reveals no burst release over the studied period of time and confirmed least free drug. Most of the loaded drug is available in the nanoscale globular body of each nanoemulsion for low and extended KTZ release at the explored pH-based media.[31] It is clear from the drug suspension that KTZ was not released after ∼4 h due to insolubility in the release medium. KTZ-ANM13 and KTZ-CNM13 executed slow and extended release over 24 h which may be attributed to slow diffusion of the drug from the nanoglobules of cationic nanoemulsion, optimal size (293 nm > 200 nm), and viscosity. Applied mathematical model suggested that KTZ-ANM13 and KTZ-CNM13 showed Fickian diffusion-controlled release (n = 0.45) at zero order release mechanism over 2 h. However, the release behavior was associated with multiple mechanisms functioning together during initial 60 min due to slight burst release and free drug. Other factors can also be taken into account such as variable globular size, cationic charge, electrostatic interaction (OLA containing primary amine for ZP reduction after partial degradation), and cationic OLA/lipid ratio during release.[32]

***Ex Vivo* Skin Permeation and Drug Retention Studies.** The results obtained from drug permeation studies of KTZ-

https://doi.org/10.1021/acsomega.2c02219
ACS Omega 2022, 7, 20267−20279

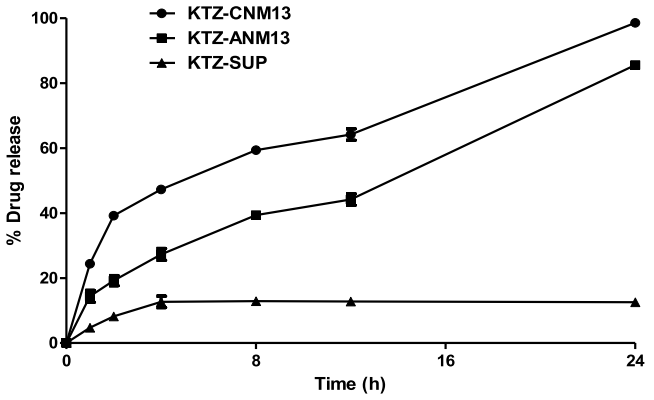

Figure 6. *In vitro* drug release (%) profile of KTZ from various formulations (KTZ-CNM13, KTZ-ANM13, and KTZ-SUP).

CNM13, KTZ-ANM13, KTZ-MKT, and KTZ-SUP are illustrated in Figure 7A. The % amount of drug permeated across rat skin was found to be 95.34 ± 1.22, 78.24 ± 1.5, 34.16 ± 2.8, and 22.76 ± 2.81 from KTZ-CNM13, KTZ-ANM13, KTZ-MKT, and KTZ-SUP, respectively, after 24 h. The permeation rate was in trend as KTZ-CNM13 > KTZ-ANM13 > KTZ-MKT > KTZ-SUP which may be envisaged based on the combined impact of formulation, positivity, and size reduction and surfactant/cosurfactant-mediated reversible changes attributed to the skin layer.[33] Moreover, low permeations from KTZ-MKT and KTZ-SUP were observed due to the conventional base-based cream and drug insolubility, respectively. KTZ-CNM13 elicited higher permeation profile as compared to KTZ-ANM13 which may primarily be attributed to the imposed cationic nature of nanoscale globules for enhanced permeation through various mechanistic phenomenon involved and working together.[18]

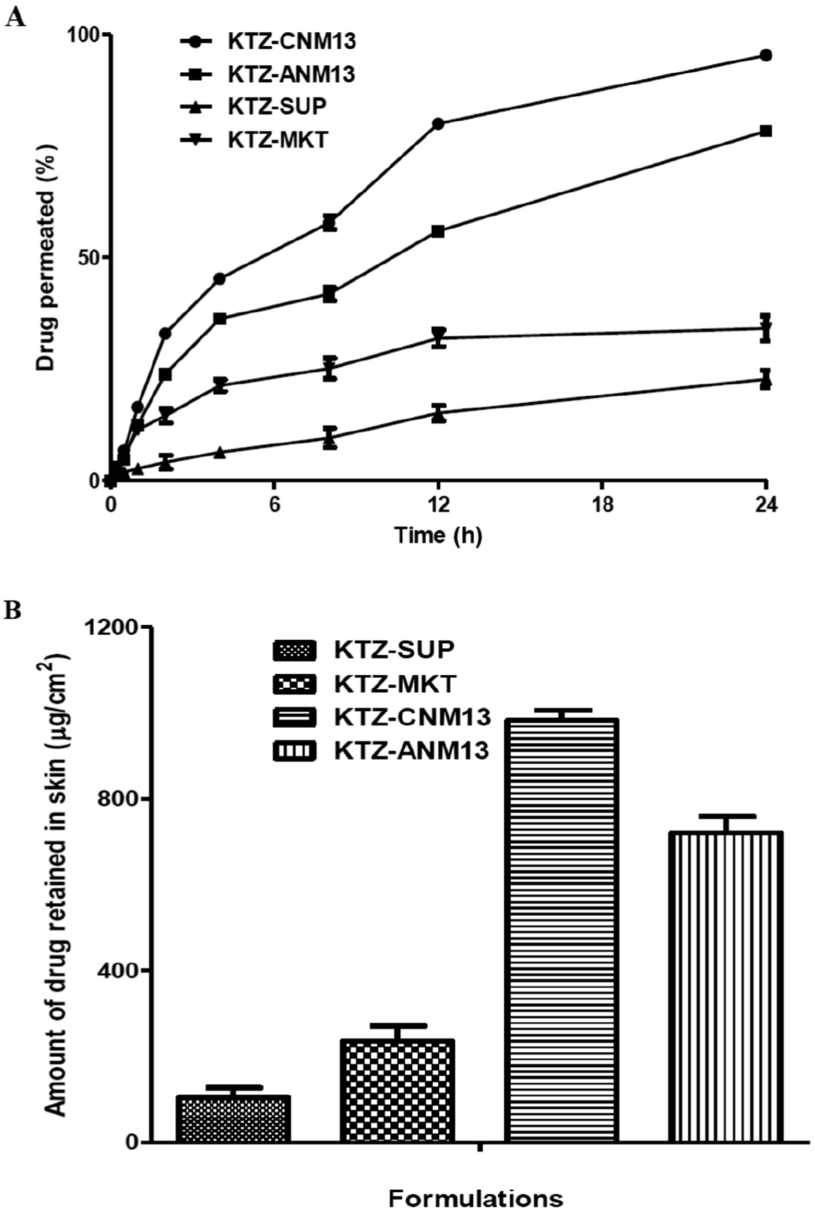

Figure 7. (A) % drug permeated study of KTZ-CNM13, KTZ-ANM13, KTZ-MKT, and KTZ-SUP for a period of 24 h using rat skin and (B) drug retention (% drug retained/cm^2) of KTZ-CNM13, KTZ-ANM13, KTZ-MKT, and KTZ-SUP after a period of 24 h using rat skin.

https://doi.org/10.1021/acsomega.2c02219
ACS Omega 2022, 7, 20267−20279

KTZ-CNM13 exhibited approximately 4 times greater permeation than KTZ-SUP. Moreover, higher permeation of KTZ-CNM13 is attributed to PG and LAB-mediated reversible perturbation and changes in the lipid-protein bilayer structure in skin layers.[27] OLA stabilized the globular construct by additional layer formation on the globular surface and subsequently prevented globules from coalescence. Being cationic in nature, it was easily internalized with negative charged skin cells for enhanced permeation and drug deposition working as a depot in the layer. Figure 7B demonstrates drug retention from KTZ-CNM13, KTZ-ANM13, KTZ-MKT, and KTZ-SUP, and these were found to be 983.4 ± 23.3, 721.29 ± 38.1, 236.31 ± 34.1, and 103.81 ± 23.3 $\mu g/cm^2$, respectively. Thus, KTZ-CNM13 illustrated maximized permeation and drug deposition after 24 h of treatment. This may be achieved due to cationic nanoscale nanoemulsion, the lowest size capable to be permeated across microscopic pores, lipid−lipid interaction between the nanoemulsion and skin lipid, surfactant-mediated reversible changes in the protein structure of the stratum corneum layer, and reduced transepidermal water loss due to hydration. Moreover, few percent of skin surface area are available for passive routes and possibly the follicular route of intracellular drug access. Such nanoemulsions have the potential to be permeated via intracellular spaces, surfactant-mediated reversible changes in the lipid bilayer of skin, paracellular pathway, and follicular route (low percent).[27] In addition, cationic nanoemulsion permeated to the dermal region is capable to be adhered around the surface of fungal cells through electrostatic interaction for maximal interaction with the cell wall, plasma membrane, and accumulation within the space below plasma membrane to toxic level resulting in cell fragmentation and cytoplasmic content oozing. Thus, this approach may produce more detrimental impact on cellular killing at a low dose (if laden with the drug for synergism) and high patient compliance.

***In Vitro* Antifungal Efficacy.** To assess the antifungal activity of various formulations, the cup and plate method was used and ZOI was measured against different strains as discussed before. The objective of adding OLA was to impose cationic charge over nanoglobules for maximized permeation and augmented fungal cellular interaction via electrostatic attraction after permeation within the tissue. Therefore, it was mandatory to have a comparative study between cationic and anionic nanoemulsion loaded with KTZ (keeping other constant). Purposely, this study studied the impact of imposed charge on nanoglobules of nanoemulsion for detrimental effect against fungal strains in *in vitro* condition, and the result is presented in Table 2. The high value of ZOI for KTZ-CNM13 against *C. albicans*, *C. glabrata*, *C. tropicalis*, and *C. krusei* as compared to KTZ-SUP can be due to the maximized interaction of cationic nanoglobules with the surface of fungal strains for extended adherence and accumulation to toxic level in the cell. As result of this, the cells are no longer alive due to developed micropores and oozing of cytoplasmic content through fragmented cell walls and plasma membrane.[34] *C. albicans* was relatively more sensitive to LAB and CAP which may be due to the innate antifungal potential of CAP and LAB.[34] Furthermore, the added sensitivity by KTZ-CNM13 can be correlated with the OA-based cationic interaction and cellular internalization (facilitated electrostatic interaction) than KTZ-ANM13 and KTZ-SUP and the drug-loaded nanoemulsion globules for facilitated adherence to the cell surface.[35] This may result in prolonged access of the drug to the fungal cell to inhibit the biosynthetic pathways of ergosterol and subsequent accumulation in the cell membrane to toxic.[36]

Table 2. *In Vitro* Antifungal Assessment of Developed Formulations Against Fungal Strains

	ZOI (mm)		
fungal strains	KTZ-SUP	KTZ-ANM13	KTZ-CNM13
C. albicans	15.2 ± 1.2	23.5 ± 1.1	34.2 ± 1.1
C. glabrata	16.3 ± 1.1	21.6 ± 1.2	38.2± 1.5
C. tropicalis	21.7 ± 1.5	25.0 ± 1.3	35.3 ± 1.8
C. krusei	19.2 ± 1.3	21.3 ± 1.1	44.2± 1.4

***In Vitro* Hemolysis Study.** This study was performed to negate the probable chance of hemolysis by the optimized formulation at the explored concentration. This would predict preliminary safety concern of the product. Permeated formulation reaching system circulation from the dermal region may cause hemolysis. However, the used excipients were of GRAS (generally regarded as safe) category and expected not to cause any sensitivity reaction and hematological crisis in systemic circulation. In general, nonionic material and natural source lipid-based product are considered to be safe and recommended for product development. Cationic and charged polymer may interact with the negatively charged RBC membrane to precipitate blood-related hematological issues. Therefore, OLA was used at low concentration for topical application. Practically, it is very difficult to eradicate fungal strain residing deep inside the dermal region of skin. This takes a longer treatment procedure and multiple drug therapy as per physician instructions (as in case of tinea treatment). The dermal region is a highly vascularized tissue and ideal for fungal growth, and it is challenging for the formulation to deliver drug there.[11] Therefore, it was necessary to impose OLA as the positive charge inducer for dual functionality at low level (0.02%) without inducing systemic hemolysis if accessed to blood circulation. This may change the cellular morphology and physiology of erythrocytes at high concentration.[37] KTZ-CNM13 and KTZ-ANM13 exhibited no marked hemolysis compared against negative as portrayed in Figure 8 wherein KTZ-CNM13 elicited the lowest % hemolysis (<12.0%) and comparable to negative control (14.3%) group (PBS 7.4). Positive control triton-X-100 caused significant lysis ($p < 0.001$) of erythrocytes and release of hemoglobin after incubation. Positive control caused 100% lysis due to its strong detergency, wettability, lipid removal properties from the lipid bilayer of biological membrane at a very low critical micelle concentration value (106−160 mg/L in water), and capable to reduce water surface tension and interfacial surface tension (between water and oil).[38] In addition, this may be due to the corrosive nature of free KTZ (azole derivative) responsible to create pores resulting in membrane destabilization.[39] To understand concentration-dependent hemolysis, maximum and minimum concentrations (1.25 and 2.5 $\mu g/mL$) were exposed to RBC suspension and incubated. The result showed no significant difference in hemolysis over explored concentration and incubation time (Figure 8). Therefore, KTZ-loaded KTZ-CNM13 could be a promising product to maximize drug access to the dermal region, improve drug efficacy, reduce emerging drug resistance,

https://doi.org/10.1021/acsomega.2c02219
ACS Omega 2022, 7, 20267−20279

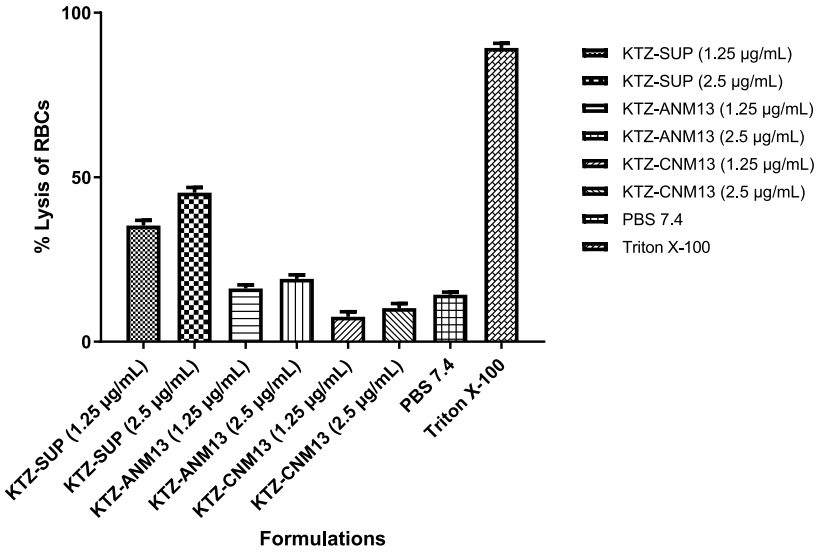

Figure 8. *In vitro* hemolysis study: KTZ-CNM13 exhibited significantly (#$p < 0.001$) low hemolysis than positive triton X-100 (10%) ($n = 3$; mean ± SD).

reduce drug cost, and ensure improve patient compliance due to reduced dose-related toxicity of KTZ (oral delivery).[40]

***In Vivo* Skin Irritation Study.** Generally, ionic polymers or surfactants in high concentration used in topical products are expected to induce dermal irritation/toxicity as a result of their binding ability to hairs and keratin protein (strong ionic bonds with the epidermal protein) of the skin surface.[41] Therefore, it was necessary to investigate the impact of KTZ-CNM13, KTZ-ANM13, and blank postapplication on the skin. The dose (0.3 mL) was applied for topical application in accordance with the earlier reported method.[11] All treated animals were closely observed and monitored for any toxicity/irritancy (redness, erythema, inflammation, and swelling), and the result was presented as score (Table 3). The obtained score was graded (scores) as per the degree of reactions (safe, mild, severe, edema, and death). Fortunately, placebo, KTZ-CNM13, and KTZ-ANM13 exhibited no abnormalities and ensured safety concern at the explored concentration of excipients and drug content. Untreated control group and treated animals were found to be free from any abnormality signs as per the visual inspection and scored graded. However, positive control showed signs of slight edema and erythema which may be due to corrosive nature of triton X100 directly applied on the skin. Notably, the successful *in vivo* performance of the nanocarrier-based formulation is associated with its *in vitro* behavior and is often affected by the rigors of formulation which it undergoes. Nanoemulsion system per se is well known to act as a cargo carrier for site-specific drug delivery and has a responsibility of protecting the drug from any instabilities both *in vitro* as well as at off target sites.[42] Cationic nanoemulsion was capable of delivering the loaded drug toward the derma region through the skin lipid extraction by the employed surfactant at concentration without causing irritation.[43]

Table 3. Acute Dermal Irritation/Corrosion Study Topical Applied of Various Formulations in Rabbits[ab]

	scores (mean value)					
	erythema			edema		
formulations	0 h	12 h	24 h	0 h	12 h	24 h
untreated	0.0	0.0	0.0	0.0	0.0	0.0
placebo KTZ-CNM13	0.0	0.1	0.1	0.0	0.0	0.0
negative control	0.0	0.0	0.0	0.0	0.0	0.0
positive control (SDS)	1.2	1.5	1.8	1.0	1.7	2.1
KTZ-CNM13	0.0	0.0	0.1	0.0	0.0	0.0
KTZ-ANM13	0.0	0.0	0.0	0.0	0.0	0.0

[a]A summary of scored report of visually inspected reactions (erythema and edema) at different time points. [b]Scores defined as 0, no erythema; 0−0.1, nonirritant and safe; 1.0−1.9, irritant; 2.0−3.0, moderate-to-severe erythema (light red); 4, severe erythema (extreme redness). SDS, sodium dodecyl sulphate.

Long-Term Study. Long-term stability results are depicted in Figure 9. The result showed that there was no significant change ($p > 0.001$) in globular size, % EE, and % drug assay when stored at 2−8 °C and 30 °C temperatures over 360 days. The % change in globular size was found as 2.5 ± 1.9, 3.8 ± 1.8, 8.2 ± 1.7, and 10.3 ± 1.5 at the end of 1, 3, 6, and 12 months, respectively, at 2−8 °C. Similar observation was obtained for unchanged particle size over a period of 3 months when the developed nanoparticle was stored at the same explored temperature and humidity by Verma et al.[44] These results were found to be as approximate values obtained from the freshly prepared product at zero day zero as there were no significance ($p > 0.001$) change. On the other hand, the values of size were observed to be slightly raised after 360 days when stored at 30 ± 2 °C/65 ± 5% RH. Notably, PDI values indicated that there was no coalescence or globular aggregation (no observed Oswald ripening like phenomenon) at both temperatures, as evidenced with no sign of phase separation and change in PDI values over the studied period. Chemical stability test confirmed the stable product at both temperatures as evidenced with % EE estimation found to be approximately unchanged over time (12 months), indicating product with a high shelf life at the explored temperatures. It is noteworthy that the gel formation was observed at an accelerated temperature (40 °C ± 75% RH), and there was significant change in all parameters, viz., globule size (80%), % EE (75%), and % drug assay (81%), possibly due to increased molecular kinetic velocity which triggered gelation, inherent nature of small globule aggregation, and transformation of solid-state behavior at higher temperature (amorphous).[45−48]

https://doi.org/10.1021/acsomega.2c02219
ACS Omega 2022, 7, 20267−20279

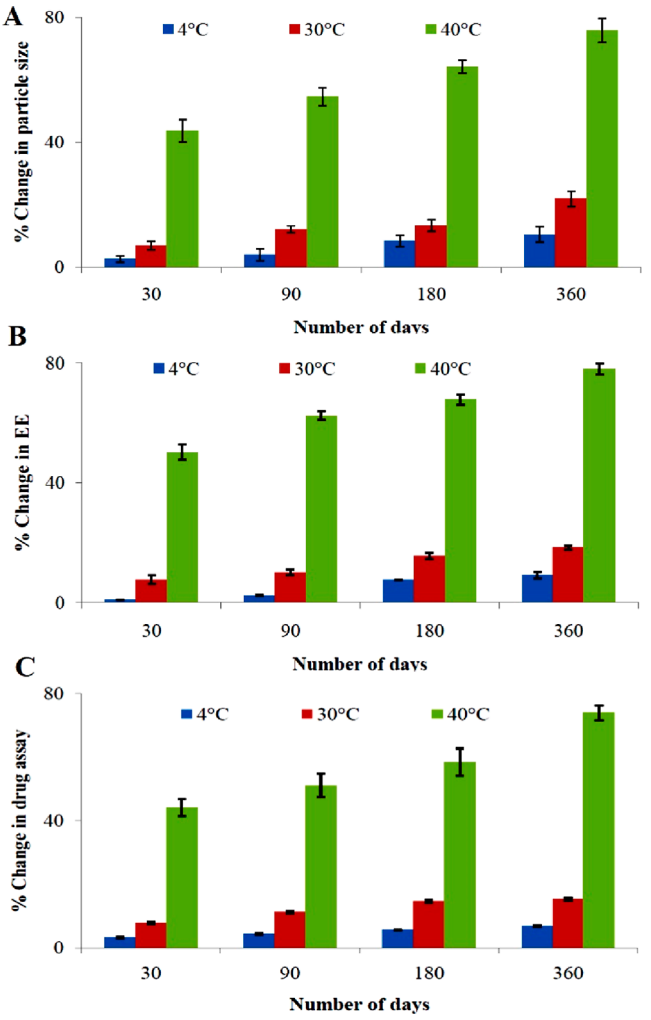

Figure 9. Effect of different temperature conditions on change in the particle size (A), % EE (B), and % TDC (C) in long-term stability studies.

CONCLUSIONS

KTZ has a broad spectrum antifungal potential to control dermal fungal infections. We hypothesized that the cationic nanoemulsion could be more detrimental due to maximum permeation, facilitated interaction with dermal cells and fungal cells, and high stability on prolonged storage. *In vitro* findings suggested that KTZ-CNM13 was the most suitable among them due to the lowest globular size, low PDI, optimal ZP, high % EE, and high % TDC. *Ex vivo* results suggested that permeation was slow and sustained to achieve therapeutic efficacy against fungal strains residing in the deeper dermal tissue. High permeation flux was achieved due to high drug deposition by KTZ-CNM13 as compared to drug suspension which can be rationalized as discussed before (through combined impact playing together). *In vitro* hemolysis confirmed the safety aspect of the product at explored concentration as preliminary toxicity assessment for topical application. ZOI values suggested the sensitivity of the product against resistant and susceptible fungi growth employing excipients possessing innate antifungal potential. Therefore, drug-laden KTZ-CNM13 showed synergism with the drug to control both the strains. Finally, *in vivo* irritation study was supportive investigation for *in vitro* hemolysis findings. Long-term stability study confirmed that the developed product using the optimized excipients was quite stable for the shelf-life period at low and room temperatures.

AUTHOR INFORMATION

Corresponding Author

Mohhammad Ramzan − *School of Pharmaceutical Sciences, Lovely Professional University, Jalandhar, Punjab 144411, India;* orcid.org/0000-0001-9029-9752; Phone: +917366800997; Email: ramzan.pharm@gmail.com

Authors

Mudassar Shahid − *Department of Pharmaceutics, College of Pharmacy, King Saud University, Riyadh 11451, Saudi Arabia*

Afzal Hussain − *Department of Pharmaceutics, College of Pharmacy, King Saud University, Riyadh 11451, Saudi Arabia;* orcid.org/0000-0002-6275-5375

Azmat Ali Khan − *Pharmaceutical Biotechnology Laboratory, Department of Pharmaceutical Chemistry, College of Pharmacy, King Saud University, Riyadh 11451, Saudi Arabia;* orcid.org/0000-0001-5955-3783

Ahmed L. Alaofi − *Department of Pharmaceutics, College of Pharmacy, King Saud University, Riyadh 11451, Saudi Arabia*

Amer M. Alanazi − *Pharmaceutical Biotechnology Laboratory, Department of Pharmaceutical Chemistry, College of Pharmacy, King Saud University, Riyadh 11451, Saudi Arabia*

Mohammad M. Alanazi − *Pharmaceutical Biotechnology Laboratory, Department of Pharmaceutical Chemistry, College of Pharmacy, King Saud University, Riyadh 11451, Saudi Arabia*

Mohd Ahmar Rauf − *Department of Pharmacy, Eugene Applebaum, College of Pharmacy and Health Sciences, Wayne State University, Detroit, Michigan 48201, United States*

Complete contact information is available at: https://pubs.acs.org/10.1021/acsomega.2c02219

Author Contributions

M.S.: conceptualization and method; A.H.: drafting, data curation, and review; A.A.K.: funding and administration; M.R.: conceptualization, software, and writing-original draft preparation; A. L.A.: formal review and editing; A.M.A.: data curation, methodology, and reviewing; M.M.A.: review and resources; M.A.R.: software, drafting, and review. All authors have read and agreed to the published version of the manuscript.

Funding

This work was funded by the Researchers Supporting Project no. (RSP-2021/339) King Saud University, Riyadh, Saudi Arabia.

Notes

The authors declare no competing financial interest.
Institutional review board statement: The study was conducted according to the guidelines of the Declaration of Helsinki and approved by the Institutional Review Board (or Ethics Committee) of Department of Institutional Ethical Committee (Panjab University, regd. no.45/GO/ReBiBt/S/99/CPCSEA)

https://doi.org/10.1021/acsomega.2c02219
ACS Omega 2022, 7, 20267−20279

and approved for the study as per ARRIVE guidelines. The protocol was followed as per ARRIVE guidelines.

■ ACKNOWLEDGMENTS

This work was funded by the Researchers Supporting Project no. (RSP-2021/339) King Saud University, Riyadh, Saudi Arabia.

■ REFERENCES

(1) Song, G.; Liang, G.; Liu, W. Fungal Co-infections associated with global COVID-19 pandemic: a clinical and diagnostic perspective from China. *Mycopathologia* **2020**, *185*, 599−606.
(2) Bongomin, F.; Gago, S.; Oladele, R.; Denning, D. Global and multi-national prevalence of fungal diseases—estimate precision. *J. Fungi* **2017**, *3*, 57.
(3) Durden, F. M.; Elewski, B. Fungal infections in HIV-infected patients. *Semin. Cutaneous Med. Surg.* **1997**, *16*, 200−212.
(4) Faergemann, J.; Baran, R. Epidemiology, clinical presentation and diagnosis of onychomycosis. *Br. J. Dermatol.* **2003**, *149*, 1−4.
(5) Shivakumar, H. N.; Juluri, A.; Desai, B. G.; Murthy, S. N. Ungual and transungualdrug delivery. *Drug Dev. Ind. Pharm.* **2012**, *38*, 901−911.
(6) Hafeez, F.; Hui, X.; Chiang, A.; Hornby, S.; Maibach, H. Transungual delivery of ketoconazole using novel lacquer formulation. *Int. J. Pharm.* **2013**, *456*, 357−361.
(7) Dave, V.; Sharma, S.; Yadav, R. B.; Agarwal, U. Herbal liposome for the topical delivery of ketoconazole for the effective treatment of seborrheic dermatitis. *Appl. Nanosci.* **2017**, *7*, 973−987.
(8) Shirsand, S.; Kanani, K.; Keerthy, D.; Nagendrakumar, D.; Para, M. Formulation and evaluation of Ketoconazole niosomal gel drug delivery system. *Int. J. Pharm. Invest.* **2012**, *2*, 201−207.
(9) Ramasamy, T.; Khandasami, U. S.; Ruttala, H.; Shanmugam, S. Development of solid lipid nanoparticles enriched hydrogels for topical delivery of anti-fungal agent. *Macromol. Res.* **2012**, *20*, 682−692.
(10) Ramzan, M.; Gourion-Arsiquaud, S.; Hussain, A.; Gulati, J. S.; Zhang, Q.; Trehan, S.; Puri, V.; Michniak-Kohn, B.; Kaur, I. P. In vitro release, ex vivo penetration, and in vivo dermatokinetics of ketoconazole-loaded solid lipid nanoparticles for topical delivery. *Drug Delivery Transl. Res.* **2022**, *12* (7), 1659−1683. Online ahead of print
(11) Ramzan, M.; Kaur, G.; Trehan, S.; Agrewala, J. N.; Michniak-Kohn, B. B.; Hussain, A.; Mahdi, W. A.; Gulati, J. S.; Kaur, I. P. Mechanistic evaluations of ketoconazole lipidic nanoparticles for improved efficacy, enhanced topical penetration, cellular uptake (L929 and J774A.1), and safety assessment: In vitro and in vivo studies. *J. Drug Delivery Sci. Technol.* **2021**, *65*, 102743.
(12) Walvekar, P.; Gannimani, R.; Salih, M.; Makhathini, S.; Mocktar, C.; Govender, T. Self-assembled oleylamine grafted hyaluronic acid polymersomes for delivery of vancomycin against methicillin resistant Staphylococcus aureus (MRSA). *Colloids Surf., B* **2019**, *182*, 110388.
(13) Teixeira, H.; Mattos, C.; Koester, L.; Bassani, V.; Argenta, D.; Misturini, F.; Simoes, C. Factorial design applied to the optimization of lipid composition of topical antiherpetic nanoemulsions containing isoflavone genistein. *Int. J. Nanomed.* **2014**, *9*, 4737.
(14) Rabinovich-Guilatt, L.; Couvreur, P.; Lambert, G.; Dubernet, C. Cationic vectors in ocular drug delivery. *J. Drug Targeting* **2004**, *12*, 623−633.
(15) Hussain, A.; Altamimi, M. A.; Alshehri, S.; Imam, S. S.; Shakeel, F.; Singh, S. K. Novel Approach for Transdermal Delivery of Rifampicin to Induce Synergistic Antimycobacterial Effects Against Cutaneous and Systemic Tuberculosis Using a Cationic Nanoemulsion Gel. *Int. J. Nanomed.* **2020**, *15*, 1073−1094.
(16) Dukovski, B. J.; Bračko, A.; Šare, M.; Pepić, I.; Lovrić, J. J. In vitro evaluation of stearylamine cationic nanoemulsions for improved ocular drug delivery. *Acta Pharm.* **2019**, *69*, 621−634.
(17) Lallemand, F.; Daull, P.; Benita, S.; Buggage, R.; Garrigue, J.-S. Successfully Improving Ocular Drug Delivery Using the Cationic Nanoemulsion. *Novasorb. Journal of Drug Delivery* **2012**, *2012*, 1−16.
(18) Altamimi, M. A.; Hussain, A.; Alshehri, S.; Imam, S. S.; Alnemer, U. A. Development and Evaluations of Transdermally Delivered Luteolin Loaded Cationic Nanoemulsion: In Vitro and Ex Vivo Evaluations. *Pharmaceutics* **2021**, *13*, 1218.
(19) Kumari, S.; Kumaraswamy, R. V.; Choudhary, R. C.; Sharma, S. S.; Pal, A.; Raliya, R.; Biswas, P.; Saharan, V. Thymol nanoemulsion exhibits potential antibacterial activity against bacterial pustule disease and growth promotory effect on soybean. *Sci. Rep.* **2018**, *8*, 6650.
(20) Khuroo, T.; Verma, D.; Khuroo, A.; Ali, A.; Iqbal, Z. Simultaneous delivery of paclitaxel and erlotinib from dual drug loaded PLGA nanoparticles: Formulation development, thorough optimization and in vitro release. *J. Mol. Liq.* **2018**, *257*, 52−68.
(21) Ahmad, N.; Ahmad, R.; Mohammed Buheazaha, T.; Salman AlHomoud, H.; Al-Nasif, H. A.; Sarafroz, M. A comparative ex vivo permeation evaluation of a novel 5-Fluorocuracil nanoemulsion-gel by topically applied in the different excised rat, goat, and cow skin. *Saudi J. Biol. Sci.* **2020**, *27*, 1024−1040.
(22) Isham, N.; Ghannoum, M. A. Antifungal activity of miconazole against recent Candida strains. *Mycoses* **2010**, *53*, 434−437.
(23) de Godoi, S.N.; Quatrin, P.M.; Sagrillo, M.R.; Nascimento, K.; Wagner, R.; Klein, B.; Santos, R.C.V.; Ourique, A.F. Evaluation of Stability and In Vitro Security of Nanoemulsions Containing Eucalyptus globulus Oil. *BioMed Res. Int.* **2017**, *2017*, 2723418.
(24) Alam, M. S.; Ali, M. S.; Alam, N.; Siddiqui, M. R.; Shamim, M.; Safhi, M. M. In vivo study of clobetasol propionate loaded nanoemulsion for topical application in psoriasis and atopic dermatitis. *Drug Invent. Today* **2013**, *5*, 8−12.
(25) Hussain, A.; Haque, M. W.; Singh, S. K.; Ahmed, F. J. Optimized permeation enhancer for topical delivery of 5- fluorouracil-loaded elastic liposome using Design Expert: part II. *Drug Delivery* **2016**, *23*, 1242−1253.
(26) Chebil, A.; Desbrières, J.; Nouvel, C.; Six, J.-l.; Durand, A. Ostwald ripening of nanoemulsions stopped by combined interfacial adsorptions of molecular and macromolecular nonionic stabilizers. *Colloids Surf., A* **2013**, *425*, 24−30.
(27) Shukla, T.; Pandey, S. P.; Khare, P.; Upmanyu, N. Development of ketorolac tromethamine loaded microemulsion for topical delivery using D-optimal experimental approach: Characterization and evaluation of analgesic and anti-inflammatory efficacy. *J. Drug Delivery Sci. Technol.* **2021**, *64*, 102632.
(28) Damasceno, B. P. G. L.; Dominici, V. A.; Urbano, I. A.; Silva, J. A.; Araújo, I. B.; Santos-Magalhães, N. S.; Silva, A. K. A.; Medeiros, A. C.; Oliveira, A. G.; Egito, E. S. T. Amphotericin B Microemulsion Reduces Toxicity and Maintains the Efficacy as an Antifungal Product. *J. Biomed. Nanotechnol.* **2012**, *8*, 290−300.
(29) Sharifi, F.; Jahangiri, M.; Nazir, I.; Asim, M. H.; Ebrahimnejad, P.; Hupfauf, A.; Gust, R.; Bernkop-Schnürch, A. Zeta potential changing nanoemulsions based on a simple zwitterion. *J. Colloid Interface Sci.* **2021**, *585*, 126 S0021979720315708−.
(30) Harris, R. A.; Shumbula, P. M.; van der Walt, H. Analysis of the Interaction of surfactants oleic acid and oleylamine with iron oxide nanoparticles through molecular mechanics modeling. *Langmuir* **2015**, *31*, 3934−3943.
(31) Shaikh, N. M.; Vijayendra Swamy, S. M.; Narsing, N. S.; Kulkarni, K. B. Formulation and evaluation of nanoemulsion for topical application. *J. Drug Delivery Ther.* **2019**, *9*, 370−375.
(32) Hagigit, T.; Nassar, T.; Beharcohen, F.; Lambert, G.; Benita, S. The influence of cationic lipid type on in-vitro release kinetic profiles of antisense oligonucleotide from cationic nanoemulsions. *Eur. J. Pharm. Biopharm.* **2008**, *70*, 248−259.
(33) Leite-Silva, V. R.; Liu, D. C.; Sanchez, W. Y.; Studier, H.; Mohammed, Y. H.; Holmes, A.; Becker, W.; Grice, J. E.; Benson, H. A.; Roberts, M. S. Effect of flexing and massage on in vivo human skin penetration and toxicity of zinc oxide nanoparticles. *Nanomedicine* **2016**, *11*, 1193−1205.

https://doi.org/10.1021/acsomega.2c02219
ACS Omega 2022, 7, 20267−20279

(34) Singh, N.; Verma, S. M.; Singh, S. K.; Verma, P. R. P. Antibacterial action of lipidic nanoemulsions using atomic force microscopy and scanning electron microscopy on Escherichia coli. *J. Exp. Nanosci.* **2015**, *10*, 381−391.
(35) Pandey, M.; Choudhury, H.; Abdul-Aziz, A.; Bhattamisra, S. K.; Gorain, B.; Carine, T.; Wee Toong, T.; Yi, N. J.; Win Yi, L. Promising Drug Delivery Approaches to Treat Microbial Infections in the Vagina: A Recent Update. *Polymers* **2020**, *13*, 26.
(36) Deschênes, L.; Ells, T. Bacteria-nanoparticle interactions in the context of nanofouling. *Adv. Colloid Interface Sci.* **2020**, *277*, 102106.
(37) Muzykantov, V. R. Drug delivery by red blood cells: vascular carriers designed by mother nature. *Expert Opin. Drug Delivery* **2010**, *7*, 403−427.
(38) Abu-Ghunmi, L.; Badawi, M.; Fayyad, M. Fate of Triton X-100 Applications on Water and Soil Environments: A Review. *J. Surfactants Deterg.* **2014**, *17*, 833−838.
(39) Thamban Chandrika, N.; Shrestha, S. K.; Ngo, H. X.; Howard, K. C.; Garneau-Tsodikova, S. Novel fluconazole derivatives with promising antifungal activity. *Bioorg. Med. Chem.* **2018**, *26*, 573−580.
(40) Gandhi, J.; Suthar, D.; Patel, H.; Shelat, P.; Parejiya, P. Development and characterization of microemulsion based topical gel of essential oil of clove (Syzygium aromaticum) for superficial fungal infections. *Adv. Tradit. Med.* **2021**, *21*, 519−534.
(41) Bujak, T.; Nizioł-Łukaszewska, Z.; Ziemlewska, A. Amphiphilic cationic polymers as effective substances improving the safety of use of body wash gels. *Int. J. Biol. Macromol.* **2020**, *147*, 973−979.
(42) Padhi, S.; Mirza, M. A.; Verma, D.; Khuroo, T.; Panda, A. K.; Talegaonkar, S.; Khar, R. K.; Iqbal, Z. Revisiting the nanoformulation design approach for effective delivery of topotecan in its stable form: an appraisal of its in vitro Behavior and tumor amelioration potential. *Drug Delivery* **2015**, *23*, 2827−2837.
(43) Verma, D.; Tahir, K.; Sushama, T.; Zeenat, I. Investigation of ethosomes as surrogate carriers for bioactives. *Drug Dev. Ther.* **2016**, *7*, 125.
(44) Verma, D.; Thakur, P. S.; Padhi, S.; Khuroo, T.; Talegaonkar, S.; Iqbal, Z. Design expert assisted nanoformulation design for co-delivery of topotecan and thymoquinone: Optimization, in vitro characterization and stability assessment. *J. Mol. Liq.* **2017**, *242*, 382 S0167732217317294−.
(45) Souto, E. B.; Müller, R. H. SLN and NLC for topical delivery of ketoconazole. *J. Microencapsulation* **2005**, *22*, 501−510.
(46) Khuroo, T.; Verma, D.; Khuroo, A.; Ali, A.; Iqbal, Z. Simultaneous delivery of paclitaxel and erlotinib from dual drug loaded PLGA nanoparticles: Formulation development, thorough optimization and in vitro release. *J. Mol. Liq.* **2018**, *257*, 52−68.
(47) Anzar, N.; Mirza, M. A.; Anwer, K.; Khuroo, T.; Alshetaili, A. S.; Alshahrani, S. M.; Meena, J.; Hasan, N.; Talegaonkar, S.; Panda, A. K.; Iqbal, Z. Preparation, evaluation and pharmacokinetic studies of spray dried PLGA polymeric submicron particles of simvastatin for the effective treatment of breast cancer. *J. Mol. Liq.* **2018**, *249*, 609 S0167732217343489−.
(48) Hamideh, A.; Rahman, Z.; Dharani, S.; Khuroo, T.; Mohamed, E. M.; Nutan, M. T. H.; Reddy, I. K.; Khan, M. A. Preparation and characterization of dicarboxylic acids salt of aripiprazole with enhanced physicochemical properties. *Pharm. Dev. Technol.* **2021**, *26*, 455−463.

https://doi.org/10.1021/acsomega.2c02219
ACS Omega 2022, 7, 20267−20279